New Results from *Chandra* Grating Observations of AGN

Tahir Yaqoob[a] [b], Urmila Padmanabhan [a]

[a]Department of Physics and Astronomy, Johns Hopkins University, 3400 N. Charles Street, Baltimore, MD 21218, USA.

[b]NASA/GSFC, Laboratory for High Energy Astrophysics, Greenbelt, MD 20771, USA.

We present measurements of the Fe-Kα line for nine type I active galaxies using *Chandra* High Energy Transmission Grating Spectrometer (*HETGS*) data. The centroid energies are narrowly dispersed (6.403 ± 0.062 keV) and indicate an origin of the *main* line peak in cold matter (Fe XVII or lower). There may be contributions from higher ionization states to the total line profile but these are not discussed here. If *all* the line cores in this sample were the peaks of a relativistically broadened disk line the radial line emissivity law must be flat and the disk inclination angles must have a restricted range. At least three of the nine AGN clearly show a complex Fe-Kα line with an underlying broad component, possibly from a disk. In the others, an apparently narrow Fe-Kα line (even if it is resolved by *Chandra*) may still be due to the peak of a disk line. To distinguish this scenario from an origin in distant matter requires variability information.

1. Introduction

The Fe-Kα emission lines in type 1 AGN can be complex, consisting of a broad ($\sim 10,000 - 100,000$ km s^{-1} FWHM) and/or a narrow ($< 10,000$ km s^{-1} FWHM) component (e.g. Yaqoob et al. 2002). The broad component probably originates from the accretion disk, having suffered severe Doppler and gravitational energy shifts in the inner disk (e.g. see reviews by Fabian et al. 2000; Reynolds & Nowak 2003) and has been clearly observed by *ASCA*. *Chandra* and *XMM* are revealing that a narrow-line (NL) component is quite common in type 1 AGN (Reeves et al. 2001; Yaqoob et al. 2001a; Yaqoob et al. 2001b; Kaspi et al. 2001; Pounds et al. 2001; Turner et al. 2002, Fang et al. 2002), often superimposed on top of a broad component. Even with *Chandra*, the NL component has only been resolved in two cases at $> 99\%$ confidence (NGC 3783 [Kaspi et al. 2002] and MCG $-6-30-15$ [Lee et al. 2002]). Interpreting the line width in NGC 3783 (1720 ± 360 km s^{-1} FWHM) as the result of Doppler shifts in a spherical gas distribution with Keplerian velocity places its origin in between the BLR and NLR. However, variability information is required to truly constrain the origin of the line. The NL observed in MCG $-6-30-15$ has a width of ~ 3600 km s^{-1} FWHM (high flux state) but it cannot arise from distant matter, as demonstrated by the rapid variability of the line (Lee et al. 2002). Thus, some of the narrow lines observed by *Chandra* could be the cores of an underlying broad disk line. Here we examine the data from nine type I AGN observed by the *Chandra HETGS*.

2. Method

The analysis method was similar to that used in Yaqoob et al. (2001a) except that the data were reprocessed using `ciao 2.1.3` and `CALDB` version 2.7, according to recipes described in `ciao 2.1.3`. The *HETGS* is composed of the *High Energy Grating* (HEG) and the *Medium Energy Grating* (MEG) and we used only the HEG data since it has the best energy resolution (1860 km s^{-1} FWHM at 6.4 keV) in the Fe-K region. We fitted the HEG data with a model of a simple power law plus a Gaussian from 2 keV to 7 keV. All parameters, including the line width, were allowed to float. The power-law slope was then frozen at the best-fit value. Using just the 5 to 7 keV data, the joint confidence contour plots of the line intensity versus the line energy, and EW versus the FWHM were made. These are shown in Figures 1 and 2 respectively. The C-statistic was used, and best-fitting line parameters, with statistical errors corresponding to 68% confidence for three interesting parameters ($\Delta C = 3.506$), are shown in Table 1. The statistical errors are a little larger than those which would be obtained for 90% confidence for one interesting parameter ($\Delta C = 2.706$). Note that the results obtained

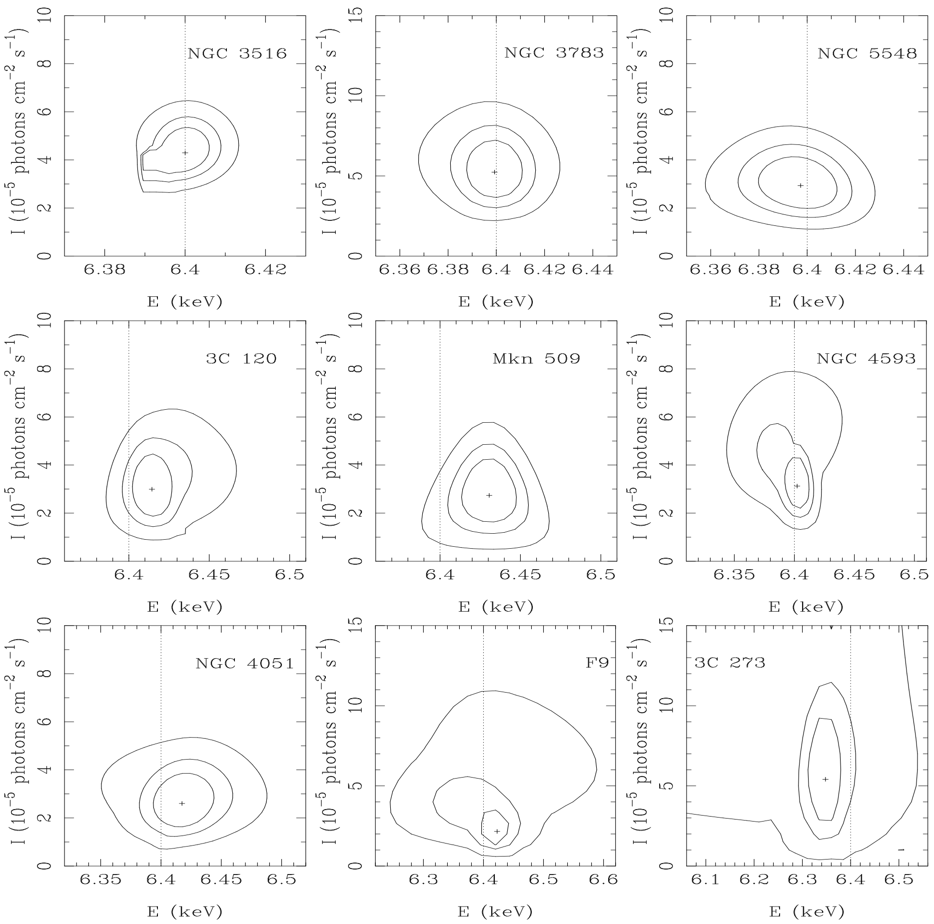

Figure 1. HEG confidence contours (68%, 90%, 99%) of intensity versus center energy when the Fe-K line cores are modeled with single Gaussians.

when the power-law slope is allowed to float are similar (full details will be presented elsewhere).

3. Centroid Energies of the Fe-K lines

In Figure 1 we show the line intensity versus line center energy confidence contours. Note that the dotted line is at 6.4 keV and all the contours intersect it, at least at the 99% confidence level. Due to the superb energy resolution of the *Chandra* HEG, the 90%, one-parameter statistical errors on the line energy can be as small as 10 eV. The most tightly constrained contours are those of NGC 3516, which has an exposure time of 100 ks and a comparatively low (2−10 keV) flux of 2.5×10^{-11} erg cm^{-2} s^{-1}. The weighted mean centroid energy of the line detected in the nine Seyfert galaxies is 6.403 ± 0.062 keV. The small dispersion is quite remarkable. If all these lines were from a disk, the line emission must be universally dominated by the largest radii. This could be achieved with a uniform illumination (per unit area) of the disk, or at least a radial illumination/emissivity law which is not steeper than r^{-2}. In that case, the larger area at larger radii will make the total line emission from the larger radii dominate over the smaller radii. See also Sulentic *et al.* (1998) for a discussion of the implications of the measurements of peak energies of the Fe-K lines. Whatever the origin of the lines, the cores observed by the HEG are formed in cold Fe (ionization states lower than Fe XVII or so).

The detailed shapes of the contours carry additional information about the line profiles, *which are not Gaussian.* Comparing the contours of NGC 5548 and F 9, we see a clear and marked difference in their contours. The 99% contours for NGC 5548 span less than ∼ 80 eV in the

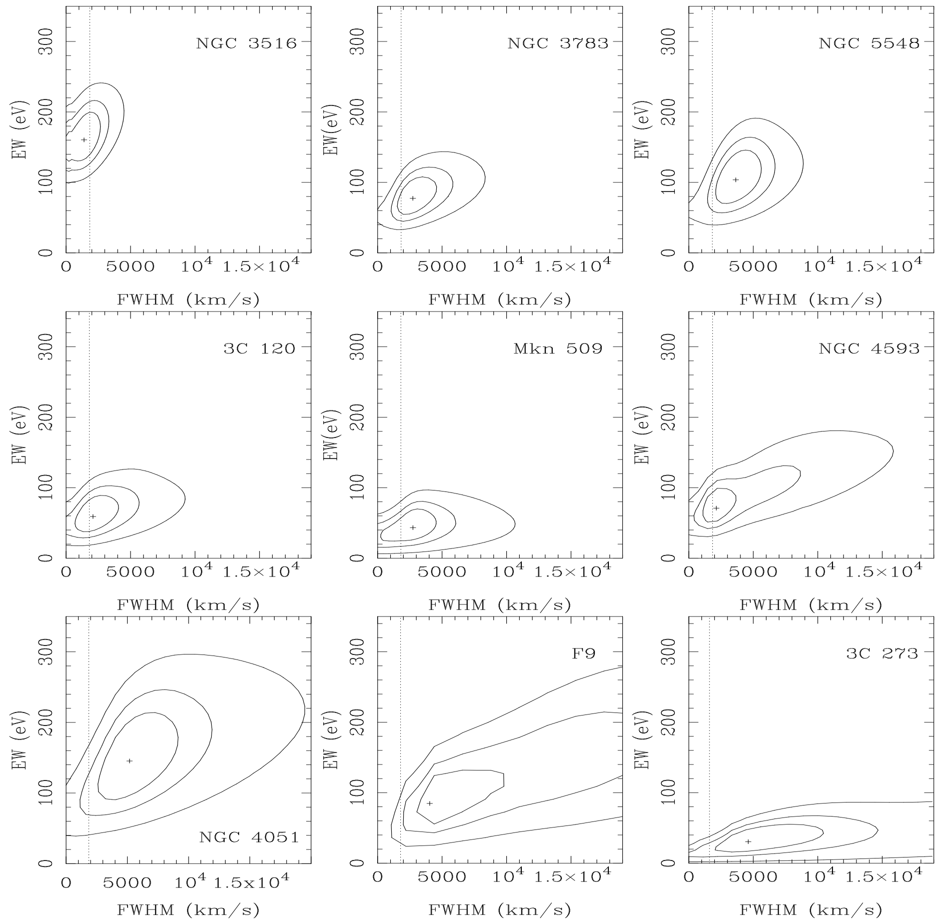

Figure 2. HEG confidence contours (68%, 90%, 99%) of EW vs. FWHM when the Fe-K line cores are modeled with single Gaussians.

line center energy, but those for F 9 span nearly 400 eV. However, the data for NGC 5548 and F 9 *have a similar signal-to-noise ratio (SNR)*, as evidenced by the similar number of photons in the 5 to 7 keV band (1240 and 1146 for NGC 5548 and F 9 respectively). Thus, the difference in the contours are due to the intrinsic differences in their line profiles and *are not due to SNR effects.* The broader contours of F 9 indicate a complex line, consistent with the line profile in Yaqoob et al. (2001b). *RXTE* data, simultaneous with the *Chandra* observation for F 9, indicates the presence of a broad line peaking at a different energy to the line measured by *Chandra* (see §5). The SNR in the other seven AGN is greater than that of NGC 5548 and F 9. Therefore, we can infer that the differences in the contours of *all* the AGN are not due to SNR effects, except for 3C 273 where the EW of the line is much less than in the other sources. The contours for NGC 3516, NGC 3783, 3C 120 and Mrk 509 are very similar to those for NGC 5548 (i.e. relatively narrow), and those for NGC 4051 and NGC 4593 are similar to those for F 9 (i.e. indicative of a broad line).

4. EW versus FWHM

In Figure 2 the EW versus FWHM confidence contours are shown. Note that the dotted line on these plots shows the FWHM resolution of the HEG (1860 km s^{-1} at 6.4 keV for $z = 0$) at the measured, *observed* peak energy of each line (that is, accounting for redshift). Again, comparing NGC 5548 and F 9 (since they have similar SNR), we find that their contours have very different shapes. The contours of NGC 5548 show the 99% confidence level (CL) FWHM upper bound at $\sim$ 10,000 km s^{-1} with the line peak unresolved

Table 1

Power law plus Gaussian fits to the *Chandra* (HEG) data.

Source	E[a] (keV)	I[b] (10^{-5} photons cm^{-2} s^{-1})	EW[c] (eV)	FWHM (*km* s^{-1})
NGC 3516[d]	$6.400^{+0.008}_{-0.010}$	$4.3^{+1.3}_{-1.1}$	162^{+47}_{-41}	1390^{+1640}_{-1390}
NGC 3783[e]	$6.399^{+0.013}_{-0.013}$	$5.3^{+2.2}_{-1.8}$	79^{+33}_{-27}	2640^{+2200}_{-1265}
NGC 5548	$6.397^{+0.021}_{-0.022}$	$3.0^{+1.5}_{-1.3}$	106^{+53}_{-46}	3650^{+2690}_{-2000}
3C 120	$6.414^{+0.019}_{-0.016}$	$3.0^{+1.8}_{-1.4}$	61^{+36}_{-29}	2090^{+2860}_{-1920}
Mrk 509	$6.431^{+0.027}_{-0.023}$	$2.8^{+1.9}_{-1.7}$	45^{+30}_{-27}	2740^{+2630}_{-2740}
NGC 4593	$6.402^{+0.014}_{-0.020}$	$3.2^{+1.5}_{-1.3}$	73^{+35}_{-29}	2140^{+4030}_{-1480}
NGC 4051	$6.417^{+0.035}_{-0.031}$	$2.7^{+1.6}_{-1.3}$	147^{+86}_{-69}	5190^{+5530}_{-3540}
F 9	$6.424^{+0.031}_{-0.089}$	$2.2^{+2.9}_{-1.1}$	86^{+113}_{-43}	4040^{+15720}_{-1840}
3C 273[e]	$6.348^{+0.052}_{-0.048}$	$5.5^{+5.9}_{-1.5}$	32^{+35}_{-9}	4610^{+8050}_{-4170}

Statistical errors are for 68% confidence for three interesting parameters ($\Delta C = 3.506$). [a] Center energy of Gaussian line. [b] Line Intensity. [c] Equivalent Width. [d] Apr 2001 obs. [e] Jan 2000 obs.

at the 99% CL. On the other hand, in F 9 the FWHM extends out $\sim$ 60,000 km s^{-1} at the 99% CL (which is off the scale in Figure 2 but can be seen in Figure 3). F 9 also shows the only resolved peak at the 99% CL in this sample. Thus, the lines in F 9 and NGC 5548 are very clearly different, with the line in F 9 definitely accompanied by a broader component and the line in NGC 5548 comparatively narrower. The FWHM contours of NGC 3516, NGC 3783, 3C 120, and Mrk 509 are similar to that of NGC 5548. NGC 4593, NGC 4051 and F 9 all show clear underlying broad components. Except for F 9, all the Fe-Kα lines in the sample, show an unresolved peak at the 99% CL.

Lee et al. (2002) found that in a *Chandra* observation of MCG $-6-30-15$, the HEG Fe-Kα line was resolved, with a best-fit FWHM width of 11,000 km s^{-1} (time-averaged). Considering only the high flux state, the line was resolved with a best-fit FWHM width of 3600 km s^{-1}. However, this line was shown to be variable on short time scales (hundreds of seconds). Thus, this line is most probably the core of a very 'peaky' disk line, since it is impossible for either the putative obscuring torus, or even the BLR to respond to continuum variations so quickly. This demonstrates that even the AGN in our sample which show 99% CL FWHM contours less than 15,000 km s^{-1} may have Fe-Kα line cores which are from a disk and not from more distant matter.

On the other hand, for the dispersion in the line centroid energies to be so small, the radial emissivity of the disk must be very flat *and* the disk inclination angles must be small and narrowly distributed (almost face-on). To determine the dominant contribution to the line core (disk or distant matter) requires variability information. The EWs of the line cores range from $\sim$ 30 eV to $\sim$ 150 eV (see Table 1). When there is an additional broad line, as measured by a higher throughput mission (e.g. *RXTE*; see §5), the total EW can easily exceed twice this value. However, an interpretation of the EWs requires detailed physical modeling which will be presented elsewhere.

5. Simultaneous RXTE Data

Now we discuss the *Chandra* observations which were simultaneous with *RXTE* (Mrk 509, NGC 4593, F 9). The *RXTE* PCA has more than 100 times the effective area of the HEG in the Fe-K band. Although the velocity resolution at these energies is $\sim 55,000$ km s^{-1} FWHM, the PCA is excellent for studying the broad component of the Fe-K lines. If we use a simple Gaussian (with intrinsic width free) to model the line in separate instruments, the PCA will 'pick-up' more line emission than the HEG (with possibly a different centroid energy), if the line is complex.

Details of the HEG Gaussian fitting have been given above. For the PCA data, in addition to a power-law continuum and Gaussian line, we included a Compton reflection continuum (from neutral, optically-thick matter) with the 'reflection fraction' (R) free, utilizing data out to $\sim$

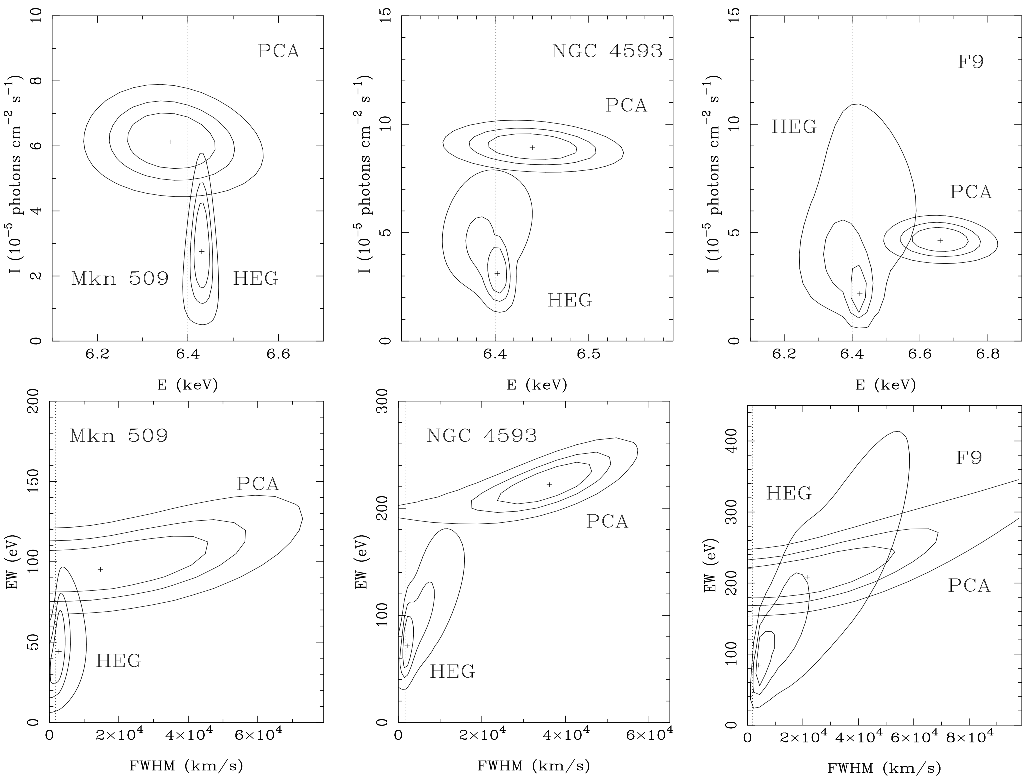

Figure 3. HEG and PCA confidence contours (68%, 90%, 99%) of Fe-K line intensity vs. center energy (top) and EW vs. FWHM (bottom).

14 – 15 keV. Figure 3 shows the 68%, 90%, and 99% confidence contours of line intensity versus centroid energy, and EW versus FWHM respectively. We defer a discussion of the derived continuua to future work. We see that for Mrk 509 the HEG and PCA give consistent results, both giving peaks at $\sim$ 6.4 keV, with the PCA giving only a marginally larger EW than the HEG. Therefore, during this observation of Mrk 509, the Fe-K line was dominated by a narrow, unresolved (by HEG) component with only a weak broad component. However, *ASCA* monitoring data of Mrk 509 showed that the peak at 6.4 keV can disappear and move to lower or higher energy, *on a timescale of days* (Weaver et al. 2001). This is puzzling and would suggest that the peak of the Fe-K line is *not* from distant matter (i.e. it is from well inside the BLR).

Next, the contours for NGC 4593 show that the HEG and PCA line intensities and EWs *do not overlap* at 99% confidence (Figure 3). Therefore the Fe-K line is definitely complex, with the HEG only picking up the core, which is about half of the intensity of the total line emission. The centroids of the HEG core and the total are both consistent with 6.4 keV, indicative of an origin in cold Fe for the whole line (i.e. ionization states lower than Fe XVII or so). Variability information is required to determine whether there are two separate line components or a single broad line.

The contours for F 9 show that the HEG and PCA measure lines with *different* centroid energies (Figure 3). We know from Mrk 509 and NGC 4593 that this is not a cross-calibration issue. In F 9 the HEG line peaks at $\sim$ 6.4 keV and the PCA line peaks at $\sim$ 6.66 keV. We caution that the PCA peak line energy for F 9 may be skewed if the continuum is different to that assumed (e.g. if the disk is ionized). We will investigate this issue in more detail in future work. Nevertheless, the *Chandra* data alone indicate a line profile which is more complex than some of the other sources. The PCA line may contain a contribution from He-like and/or H-like Fe in addition to the 6.4 keV component measured by the HEG. This time there is not a clear distinction between the HEG and PCA EW versus FWHM contours, because, as is evident from the line profile (see Yaqoob et al. 2001b), the core of the line is not as 'peaky' as that in some of the other AGN (such as Mrk 509 and NGC 4593). In fact, Figure 3 shows that the HEG contours from single-Gaussian fits pick up the whole broad line, and indeed F 9 is one of the objects in which the broad profile is detected with the HEG. Note that a narrow $\sim$ 6.4 keV Fe-K line plus a broad He-like line has been observed in *XMM* observations in at least three other AGN (Mrk 509, Mrk 205, Reeves, these proceedings; NGC 5506, Matt et al. 2001) and may be a common signature.

6. Conclusions

Measurements of the Fe-Kα line centroid energies for nine type I active galaxies using the best energy resolution available ($\sim$ 1860 km s^{-1} FWHM) show that they are narrowly dispersed (6.403 ± 0.062 keV) and are consistent with a dominant contribution *to the line core* from cold matter (ionizations states less than Fe XVII or so). Of the nine AGN, the core in only F 9 is resolved at $> 99\%$ confidence. Three sources (NGC 4051, NGC 4593 and F 9) show a complex Fe-Kα line with an underlying broad, relativistic component. In the remaining AGN we cannot rule out the line core originating in a relativistic accretion disk (as opposed to originating in distant matter). However, the small dispersion in the peak energy requires a very flat radial emissivity law and a limited range in disk inclination angle. A flat emissivity law may in fact be quite likely, especially if the disk is illuminated by an extended X-ray source, such as the disk corona. A restricted range in disk inclination angles may also not be unreasonable since type I AGN are supposed to be viewed face-on or close to face-on. Thus, narrow Fe-K lines do not necessarily imply a non-disk origin. Variability information is required to determine the origin of the line core in these cases. A further clue may be obtained from the detailed shapes of the line profiles (some of which are markedly asymmetric) obtained by the *Chandra* gratings. Details will be reported in future work.

REFERENCES

1. Fabian, A. C., Iwasawa, K., Reynolds, C. S., & Young, A. J. 2000, PASP, 112, 1145
2. Fang, T., Davis, D. S., Lee, J. C., Marshall, H. M., *et al.* 2002, ApJ, 565, 86
3. Kaspi, S. et al. 2002, ApJ, 554, 216
4. Lee, J. C., Iwasawa, K., Houck, J. C., Fabian, A. C., *et al.* 2002, ApJ, 570, L47
5. Matt, G., Guainazzi, M., Perola, G. C., Fiore, F., Nicastro, F., *et al.* 2001, A&A, 377, L31
6. McKernan, B., & Yaqoob, T. 2003, in ASP Conf. Ser., IAU Symp. 214, High Energy Processes and Phenomena in Astrophysics, ed. X.-D. Li, Z.-R. Wang, & V. Trimble (San Francisco: ASP), in press (astro-ph/0211384)
7. Reeves, J. N., Turner, M. J. L., Pounds, K. A., O'Brien, P. T., *et al.* 2001 A&A, 365, L134
8. Reynolds, C. S., & Nowak, M. A. 2003, Pys. Rep., in press (astro-ph/0212065)
9. Sulentic, J. W., Marziani, P., Zwitter, T., *et al.* 1998, ApJ, 501, 54
10. Turner, T. J. et al. 2002 ApJ, 574, L123
11. Pounds, K., Reeves, J., O'Brien, P., Page, K., Turner, M., & Nayakshin, S. 2001 ApJ, 559, 181
12. Weaver, K. A., Gelbord, J., & Yaqoob, T. 2001, ApJ, 550, 261
13. Yaqoob, T., George, I. M., Nandra, K., Turner, T. J., Serlemitsos, P. J., & Mushotzky, R. F. 2001a ApJ, 546, 759
14. Yaqoob, T. & Padmanabhan, U. 2003, in ASP Conf. Ser., Active Galactic Nuclei, from Central Engine to Host Galaxy, ed. S Collin, F. Combes & I. Shlosman, (San Francisco: ASP), p. 7 (astro-ph/0211349) [YP03]
15. Yaqoob, T., Padmanabhan, U., Dotani, T., George, I. M., Nandra, K., Tanaka, Y., Turner, T. J., & Weaver, K. A. 2001b, in Conf. Proc., X-ray Emission from Accretion onto Black Holes, Proceedings, ed. T. Yaqoob, & J. H. Krolik (published electronically on ADS), E79 (astro-ph/0111419)
16. Yaqoob, T., Padmanabhan, U., Dotani, T., & Nandra, K. 2002, ApJ, 569, 487

ACKNOWLEDGMENTS

The authors gratefully acknowledge support from NASA grants NCC-5447 (T.Y., U.P.), NAG5-10769 (T.Y.), and CXO grants GO1-2101X, GO1-2102X (T.Y.). The authors are grateful to the *Chandra* and *RXTE* instrument and operations teams for their work. We also thank our collaborators, B. McKernan, I. M. George, T. J. Turner, & K. Weaver.